Hindawi
Scientific Programming
Volume 2021, Article ID 1531724, 7 pages
https://doi.org/10.1155/2021/1531724

Research Article

Prenatal Diagnosis of Fetal Cleft Lip and Palate with Three-Dimensional Ultrasound Information Technology

Xinglong Deng, Suhui He, Qiumei Wu, Zongjie Weng, Minmin Yang, and Min Liu

Department of Ultrasound, Fujian Provincial Maternity and Children's Hospital, Fuzhou 350001, Fujian, China

Correspondence should be addressed to Min Liu; 181005103838@bitzh.edu.cn

Received 6 May 2021; Accepted 1 July 2021; Published 12 July 2021

Academic Editor: Gustavo Ramirez

Objective. To evaluate the three-dimensional ultrasound paper cleft lip and palate deformities in applications in prenatal diagnosis. *Methods*. 25 cases of cleft lip and palate fetus, 20–32 weeks of gestational age, with the maternal age of 22–44 years, were examined by prenatal ultrasound in our hospital; conventional two-dimensional ultrasound examination was performed after a cleft lip, and the application of three-dimensional ultrasound imaging surface and a transparent imaging showed the alveolar process and the palate of the fetus. Also, the results of two-dimensional ultrasound and postnatal (or after induction) results were compared. *Results*. Of the 25 cases, there were 6 cases of postpartum induction or simply unilateral cleft lip, 17 cases of unilateral cleft palate, and two cases of bilateral cleft lip palate. There was no significant ($P > 0.05$) difference of two- and three-dimensional ultrasound detection rate of pure cleft lip; two-dimensional ultrasound cleft palate detection rate was 36.8% (7/19), and three-dimensional ultrasound cleft palate detection rate was 89.5% (17/19). The two methods showed a statistically significant ($P < 0.05$) difference in the detection rate of cleft palate. *Conclusion*. Three-dimensional ultrasound can significantly improve the diagnostic accuracy of prenatal cleft palate.

1. Introduction

Cleft lip and palate deformities are facial and small organ deformities with a high prevalence, ranking 4th in fetal malformations. The neonatal incidence is 1.5% to 2.0%. Cleft lip and palate can occur alone or as one of the manifestations of multiple malformations. Its type is significantly related to fetal outcome, additional structural malformations, and chromosomal abnormalities. Cleft palate often causes respiratory infections, malnutrition, middle ear problems, etc. In severe cases, it can cause language development disorders, which has a great psychological impact on children. About 25000 newborns with cleft lip and palate are born every year in China, which is the main disease for medical identification of sick and disabled children. Prenatal diagnosis of fetal malformations is an important link to improve the quality of the birth population. In 2012, the "Prenatal Ultrasound Guidelines" formulated by the Ultrasound Physicians' Association of the Chinese Medical Doctors Association included lips in the evaluation scope of prenatal examinations. Many scholars have also reported ultrasound can detect cleft lip and palate, but there is a certain degree of difficulty of detection [1]. According to the presence or absence of fetal outcome cleft palate, surgery is difficult and critical to the treatment sequence, and we evaluate whether to terminate the pregnancy. Thus, cleft palate prenatal diagnosis is particularly important.

2. 3D Ultrasound Information Technology to Multivariate Interpolation

The multivariate interpolation problem can be expressed as follows: Given a set $X = \{X_i \in R^d, i = 1, 2, \ldots, N\}$ containing N different points and a corresponding set $Y = \{f_i \in R, i = 1, 2, \ldots, N\}$ of N real numbers, we find a function s: $R^d \longrightarrow R$ that meets the interpolation conditions:

$$s(X_i) = f_i, \quad i = 1, 2, \ldots, N. \tag{1}$$

Obviously, when $d = 2$ or 3, it means that the interpolation surface defined by s passes all the given points. The radial basis function method is one of the feasible methods to solve the abovementioned real multivariate interpolation problem. The radial function is satisfied if $\|x_1\| = \|x_2\|$; then, the function ϕ of $\phi(x_1) = \phi(x_2)$. That is, a function that depends only on $r = \|x\|$, and $\|\bullet\|$ usually represents the Euclidean norm. The radial basis function is such a function space (shown in Figure 1). A unary function ϕ: $R_+ \longrightarrow R$ in the domain $x \in R^d$ is given. All function spaces of the form $\Phi(x - c) = \phi(\|x - c\|)$ and their linear combinations are called radial basis function spaces derived from function ϕ. The radial basis function method mainly selects a function s with the following form [2]:

$$s(X) = \sum_{i=1}^{N} w_i \phi\left(\left\|X - X_i\right\|\right). \tag{2}$$

Among them, $\{\phi(\|X - X_i\|) | i = 1, 2, \ldots, N\}$ is a set of N radial basis functions, and the known data point $X_i \in R^d$, $i = 1, 2, \ldots, N$ is taken as the center of the radial basis functions.

Given the interpolation conditions (1) and (2), we get a set of linear equations about the unknown weight coefficient $\{w_i | i = 1, 2, \cdots, N\}$:

$$\begin{bmatrix} \phi_{11} & \phi_{12} & \cdots & \phi_{1N} \\ \phi_{21} & \phi_{22} & \cdots & \phi_{2N} \\ \vdots & \vdots & \vdots & \vdots \\ \phi_{N1} & \phi_{N1} & \cdots & \phi_{NN} \end{bmatrix} \begin{bmatrix} w_1 \\ w_2 \\ \vdots \\ w_N \end{bmatrix} = \begin{bmatrix} f_1 \\ f_2 \\ \vdots \\ f_N \end{bmatrix}. \tag{3}$$

Among them, $\phi_{ji} = \phi(\|X_j - X_i\|)$, $i, j = 1, 2, \ldots, N$.

Remember $F = [f_1, f_2, \ldots, f_N]^T, W = [w_1, w_2, \ldots, w_N]^T$.

$$\Phi = \begin{bmatrix} \phi_{11} & \phi_{12} & \cdots & \phi_{1N} \\ \phi_{21} & \phi_{22} & \cdots & \phi_{2N} \\ \vdots & \vdots & \vdots & \vdots \\ \phi_{N1} & \phi_{N1} & \cdots & \phi_{NN} \end{bmatrix}. \tag{4}$$

Calling Φ the interpolation matrix, the system of (3) can be abbreviated as

$$\Phi W = F. \tag{5}$$

If matrix Φ is not singular, its inverse matrix exists, and the weight coefficient vector W is solved from the abovementioned formula.

$$W = \Phi^{-1} F. \tag{6}$$

Here, a crucial question is how to ensure that matrix Φ is not singular, that is, the system of equations has a solution, and choosing a suitable radial basis function expression can completely satisfy this condition [3].

3. Materials and Methods

3.1. General Information. In this paper, 25 cases of fetuses with cleft lip and palate confirmed by postnatal or labor induction in hospital from December 2018 to October 2010 were selected. The gestational age was 20 to 32 weeks, and the pregnant women were 22 to 44 years old. The study protocol was approved by the Ethics Committee of Hospital, and the patient or his family members signed the written informed consent form.

3.2. Instruments and Methods. We used a color Doppler ultrasound system, equipped with an RAB4-8-D volume probe, frequency 4–8 MHz, and transabdominal two-dimensional probe C1-5-D, frequency 1–5 MHz, with 2D, 3D, and real-time 3D capabilities. (1) We first performed a conventional two-dimensional examination of the fetus. After obtaining the biparietal plane, we rotate 90° for a coronal plane scan and then rotate 90° for a cross-sectional scan of the nasolabial region. After showing the nostrils and upper and lower lips, we rotate 90° and a sagittal plane scan was performed with the nasal bones as the marker. (2) After the child with cleft lip is found, we started the 3D surface mode to determine the fetal cleft lip, then started the 3D transparent imaging mode, selected 3D static render mode skeleton, and collected 3D facial volume data from the sagittal plane (preferred) or oblique sagittal plane to avoid probe movement and fetal movement, the largest possible collection of lip and palate volume data. The midsagittal plane of the fetus is displayed, with the frontal and nasal bone, soft tissues, and lips as marks. We try to make pregnant women hold their breaths to reduce the impact of movement. The fetal breathing can be ignored. The probe was kept still and collected successfully after a few seconds. The volume data are stored on the machine's hard disk for postprocessing analysis.

3.3. Image Postprocessing. Three-dimensional ultrasound surface imaging can be used for real-time imaging. The probe can be moved at any time to observe fetal movement. We adjusted the size of the sampling frame so that the face is at the center and adjusted the *X*-, *Y*-, and *Z*-axis to obtain a clear facial image of the fetus. In surface imaging mode (as shown in Figure 2), sagittal, coronal, and cross sections can be viewed on the same screen by adjusting the *A*, *B*, and *C* planes. In the transparent imaging mode, we first rotate the *Z*-axis by 90° on the *A* plane, erect the sagittal section, and adjust the size and position of the sampling frame so that the sampling frame includes the lip and palate and the center point is on the alveolar ridge; on the *B* plane, *X* is rotated. The coronal or near coronal section is obtained on the *Y*- and *Y*-axis, and the orbit is used as the mark. Moving the center point on the *C* plane, we can observe the axial information of the lip and palate, that is, the alveolar bone and hard palate, and reconstruct the palate information. The rendering mode can present reconstruction, and the crotch image can be adjusted for grayscale, brightness, and transparency threshold levels to optimize image contrast and resolution between fetal bone and soft tissue (Figure 3). For the oblique sagittal plane, we first adjust the approximate sagittal plane on the *A* plane, and the rest of the adjustment is the same as that mentioned above. Orthogonal scan planes are displayed

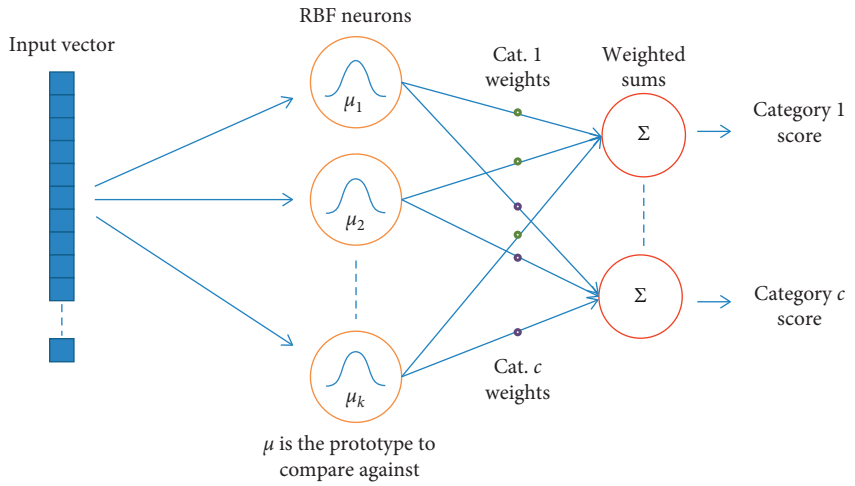

Figure 1: Radial basis function.

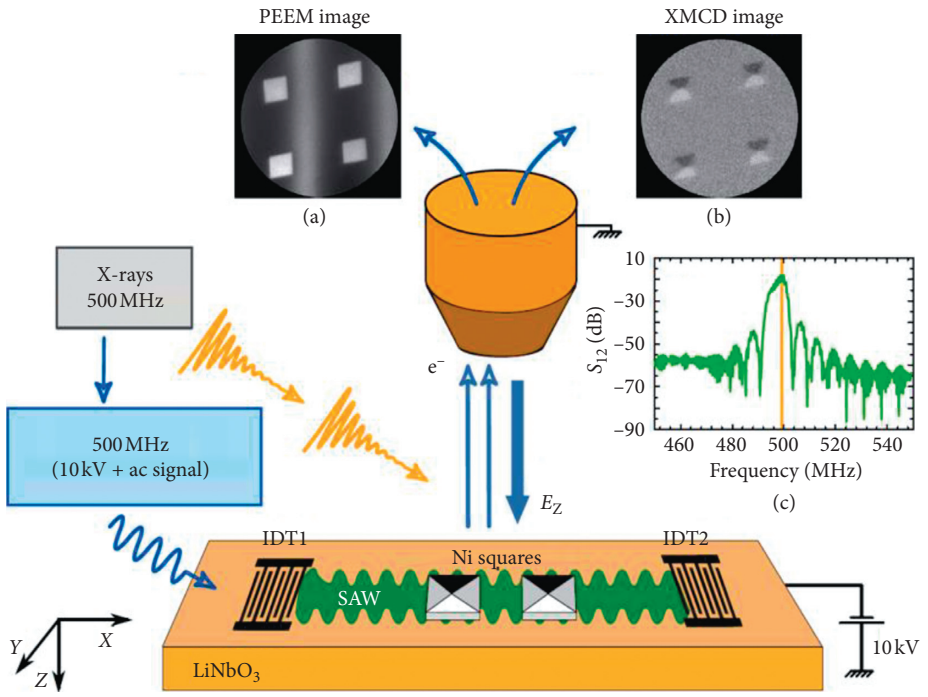

Figure 2: Surface imaging mode.

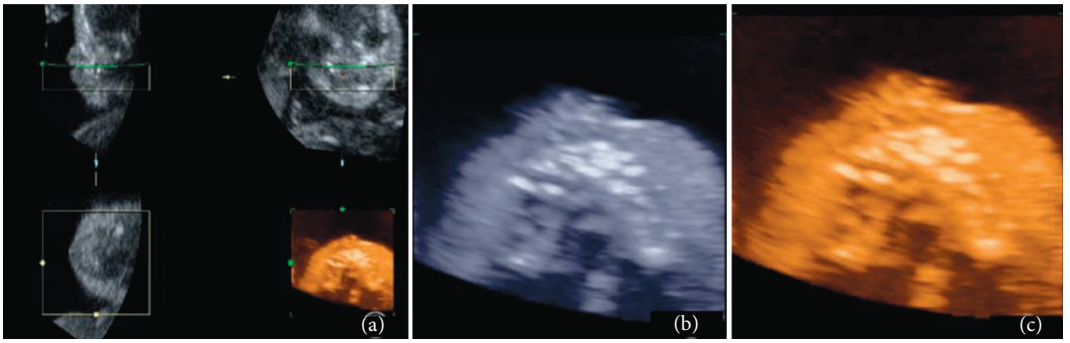

Figure 3: 3D reconstructed image of the normal fetus in the 26th week.

as standardized face views. The plane reconstruction of the sacral cross section shows yellow reference points on the *C*-shaped alveolar ridge, and the corresponding reference points also appear on the coronal and sagittal planes. If the hard palate is not clear, you can rotate it by a certain angle on the *Y*-axis, generally ≤45°.

Among them, the three-dimensional image of the crotch is reconstructed in Figure 3(a), where the upper left is a vertical sagittal plane, the upper right is a coronal plane, the lower left is an axial plane, and the lower right is a rendered image displayed after reconstruction of the crotch; Figures 3(b) and 3(c) give the enlarged image. You can adjust the color and brightness at the bottom right to increase the contrast, as in Figure 3(a).

3.4. Statistical Processing. SPSS 13.0 software was used for statistical analysis. The results were analyzed by the $\chi 2$ test. $P < 0.05$ was considered statistically significant.

4. Results

25 cases of cleft lip and palate and induction of fetal postpartum results: Six patients with unilateral simple cleft lip and cleft palate, seventeen cases of unilateral, and two cases of bilateral cleft lip palate. There was 1 case of unilateral cleft, one twin fetus, while another fetus was normal, and 1 patient with bilateral cleft lip palate of multiple malformations, ventricular septal defect, cerebellar vermis deletions, and spina bifida occulta SUA.

4.1. Two-Dimensional Sound Image Performance. In 25 cases of fetal cleft lip, the continuous line echo of the upper lip was interrupted, the echo at the broken end was enhanced, and the interruption was an echoless dark band (Figure 4(a)), which was more obvious when the mouth was opened. Nine cases had incomplete cleft lip, and the nasal shape was basically normal; 16 cases had incomplete cleft lip showing continuous upper echo interruption of the upper lip, wide gap, cracks extending to the root of the nose, asymmetric nostrils, and enlarged nasal cavity, of which 12 cases had lateral nasal collapse, nasal septum shifted to the healthy side. In the middle of the cleft lip, the upper lip and the middle cleft lip are wide, and the shape of the nose is obviously abnormal. In 7 cases of cleft lip and palate, in addition to the abovementioned signs of cleft lip, the maxillary alveolar process was discontinuous, and the normal arc was interrupted. The "dislocation sign" was seen on the cross section. In 5 cases, the alveolar fissure split between the lateral incisor and the canine, the arc-shaped strong echo of the hard palate on the side of the coronary lesion, and the soft tissue band of the medium echo of the soft palate were interrupted. On the sagittal view, the echo of the hard palate and soft palate appeared intermittently. The cleft reaches the nasal cavity. In 2 cases of bilateral cleft lip with alveolar cleft or complete cleft palate, a strong echogenic mass protruding prominently under the nose can be displayed as the anterior process of the jawbone, which is an important clue to confirm bilateral cleft lip and palate. The rift itself is easier to spot. Too much amniotic fluid and small gastric vesicles may also indicate the presence of cleft palate.

4.2. Three-Dimensional Sound Image Performance. During the cleft lip, the upper lip was interrupted continuously, and a gap was seen, which resembled "rabbit lip trilobate" (Figure 4(b)). In 16 cases, the complete cleft lip was seen extending to the root of the nose, and the lip was "eight." The shape of the nose was abnormal. The lateral nasal wing collapsed, the nasal septum shifted to the healthy side, and the nostrils were asymmetric. In 17 cases of alveolar fissures, the cross section of the multiplanar image showed a continuous interruption of the arc-shaped high echo of the alveolar process, and the gap was a low echo (Figure 4(c)); the rendered image showed a partial arc of the alveolar process with strong echo. The fissure-like hypoechoic area extending to the hard palate was interrupted (Figure 4(d)).

While the two-dimensional image of Figure 4(a) illustrates cleft lip discontinuity, interrupted anechoic dark band, Figure 4(b) illustrates reconstruction of three-dimensional surface model cleft (arrow); Figure 4(c) MPR shows the palate with alveolar hypoechoic visible cracks (center point); and in the transparent mode, Figure 4(d) illustrates a rendered image reconstructed fracture cleft (arrow).

4.3. Two-Dimensional Ultrasound and Comparison of the Three-Dimensional Ultrasound Detection Rate of Cleft Lip and Palate. There was no significance ($P > 0.05$) (Table 1) of the two-dimensional and three-dimensional ultrasound detection rate of cleft lip. A simple difference was considered a statistically significant ($P < 0.01$) difference in the detection rate of cleft lip palate.

5. Discussion

5.1. Two-Dimensional Ultrasound Detection of Fetal Cleft Lip and Palate. Currently, two-dimensional ultrasound has been able to successfully diagnose cleft lip deformity. Also, due to the acoustic shadow palate structure, the detection of the palate is more difficult, but about 85% of clinical palate cleft lip and cleft palate which was particularly important was detected, and three-dimensional ultrasound can increase the detection rate of cleft palate.

The two-dimensional ultrasound cross section is the best section to show the upper alveolar process, but it is difficult to show the integrity of the alveolar process. Sometimes, it can only be partially displayed. It is mainly affected by the position of the fetus and the scanning angle. Frequent scanning is required. Moving the probe shows from multiple sections that it lacks advantages in evaluating the relationship between the location of the lesion and the surrounding tissue structure and requires physicians to have skilled methods and rich experience. Two-dimensional ultrasound mostly relies on the indirect signs of cleft lip to diagnose cleft lip deformity: the upper lip has a gap of 0.8 cm and the nose has no abnormal shape, which is mostly a cleft lip; with the gap of >0.8 cm, the nose deforms and collapses, and when the mouth is opened, the fetal tongue extends to

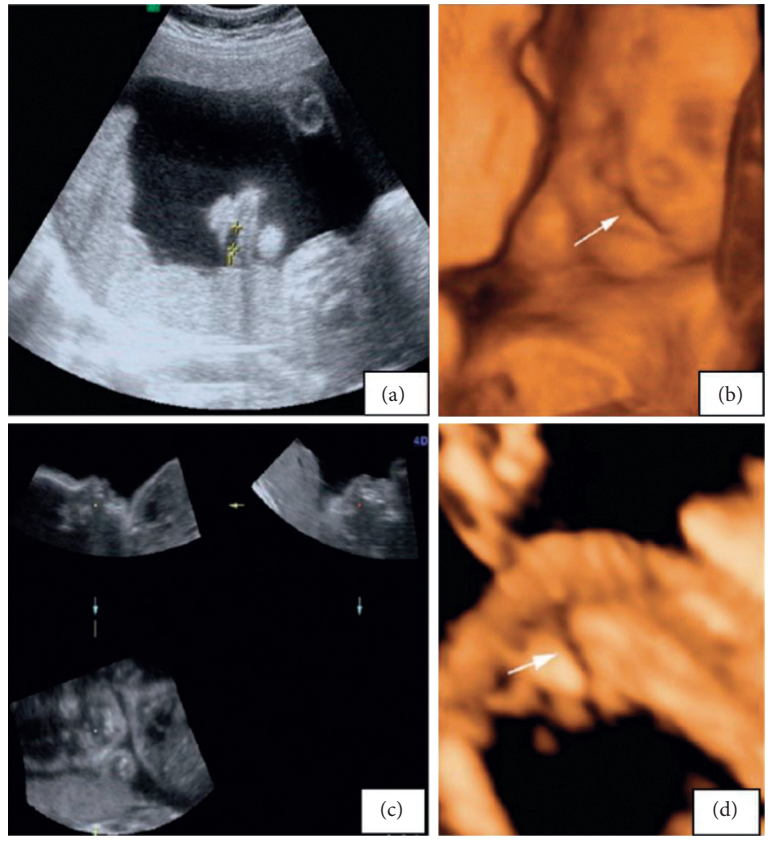

Figure 4: 25-week fetal unilateral cleft lip and palate deformity.

Table 1: Comparison of detection rates of fetal cleft lip and palate with two-dimensional and three-dimensional ultrasound.

Inspection method	Simple cleft lip	Cleft lip and cleft palate	Cleft lip and palate
Two-dimensional ultrasound	100.0 (6/6)	36.8 (7/19)	52.0 (13/25)
3D ultrasound	100.0 (6/6)	89.5 (17/19)	92.0 (23/25)

the upper lip defect. It enters the nasal cavity through the cleft and often merges with cleft palate [4].

The iliac crest is located posteriorly and inwardly of the alveolar process. Due to the obstruction of the surrounding structure, the 3D reconstruction success rate is relatively poor compared to the lips and alveolar process. In this study, 7 cases of hard palate showed unclear two-dimensional ultrasound (as shown in Figure 5). One case had a placenta at the front wall at 30 weeks of gestation. The pregnant woman had a fat body with poor image quality and could not be judged. The remaining 6 cases were complete. There was no echo area, and it could not be displayed. When adjusting the image, it is rotated by a certain angle, but the reconstructed image is still not satisfactory. It may be that the direction of the sound beam is parallel to the hard palate, and the bony alveolar process completely attenuates the sound beam and it is impossible to collect volume data of the hard palate (as shown in Figure 6, two-dimensional and three-dimensional ultrasound contrast). Therefore, only when the sound beam direction is at a certain angle or perpendicular to the hard palate, the volume data of the hard palate can be obtained and displayed through post-processing. The oblique sagittal plane can remove the influence of some alveolar bone acoustic images and improve the display rate of the palate. The image acquired through the mandibular sagittal plane has a high display rate of the hard palate reconstruction.

In this study, the display rate of hard palate was extremely low. Only when the fetal face is facing the mother's ventral side, the fetal head is tilted back, the sound beam is at an angle with the hard palate, and there is no obstruction in front of the face. It may be detected, so it is more limited. Li Shengli and others reported that the fetal palate could be detected through the submaxillary triangle, and the intrauterine fetal display rate was 5%. In [5], 8 cases of early cleft palate with high-risk fetuses and other malformations were diagnosed by observing the integrity of the line under the nasal triangle of the fetus from 11 to 14 weeks of gestation. Because there are too few cases during early pregnancy, more clinical studies are still needed to confirm the integrity of the posterior nasal triangle for diagnosis of cleft palate. In [6], 2D and 3D ultrasound were used to systematically check 3,598 fetuses. 11 cases (0.31%) of simple cleft palate were detected, and 1 case was missed. The coronal section, maxillary cross section, median sagittal section, peroral fissure oblique crown section, etc., were observed.

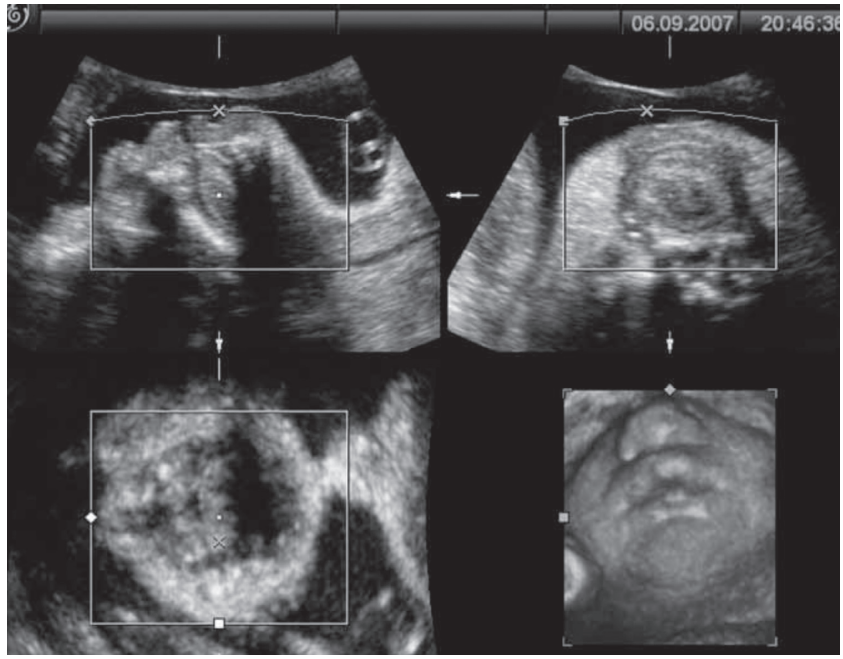

Figure 5: Unclear display of two-dimensional ultrasound of hard palate.

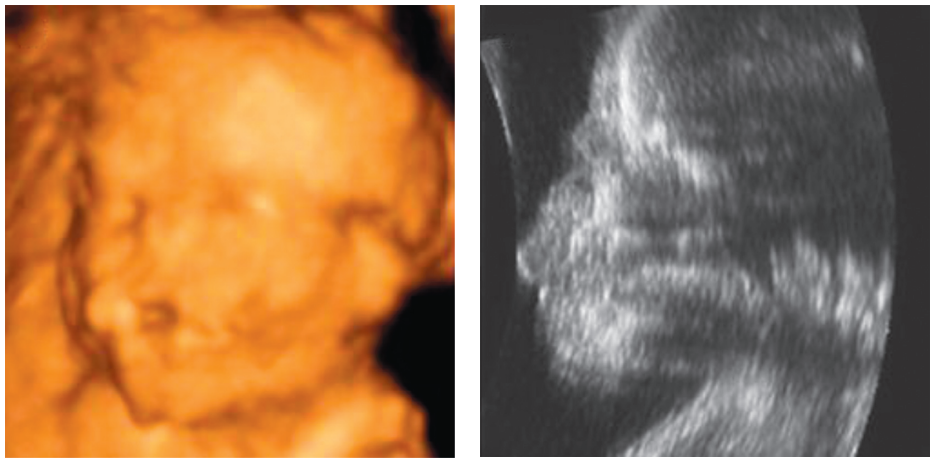

(a) (b)

Figure 6: Comparison of 2D and 3D ultrasound.

5.2. Three-Dimensional Ultrasound Detection of Fetal Cleft Lip and Palate. Three-dimensional surface mode imaging for the detection of cleft lip deformities is more intuitive and easier to be accepted by patients and their families. The transparent mode can observe fetal bone structures, such as the spine, thorax, and long bones of the extremities. In this study, the surface mode was used to observe the shape and integrity of the nose and lips, and the multiplanar mode and transparent imaging were used to observe the continuity of the maxilla, the alveolar process, and the hard palate. He Guangzhi and others applied three-dimensional ultrasound free anatomy imaging technology to analyze the volume data of 100 normal fetuses through the midsagittal section of the mandibular face. It was found that three-dimensional ultrasound is easy to operate compared to the two-dimensional ultrasound which has difficultly in displaying and reduces the operator's skills and experience dependency. Li Xia and others used three-dimensional surface imaging and volume contrast imaging to observe and study the palate [7]. They believed that three-dimensional ultrasound can improve the sensitivity, specificity, and specificity of diagnosing cleft lip and palate and reduce the rate of missed diagnosis.

In this study, three-dimensional transparent imaging was used to observe the fetal condyle. For fetuses with suitable conditions, only a few seconds of satisfactory volume data can be collected and postprocessed. Three-dimensional imaging makes it easier to identify the maxilla and the mandible, and distinguishing between the maxilla and the mandible is very important in diagnosis. Maxillary

alveolar ridges are often affected by cleft palate. The three-dimensional imaging sagittal section can interactively display the corresponding side axial view of the fetal face, thereby minimizing this potential error. Three-dimensional imaging may be viewed in three mutually perpendicular facets in the shape and size of the fracture and the range involving the relationship with the surrounding tissue structure and confirm each other in a three section, avoiding the misdiagnosis simply using a single slice, or may cause missed diagnosis. Like the anatomical atlas, nose shape and the three-dimensional image reconstructed cleft can also be observed so that the visual image can more accurately determine whether or cleft, present location and range involved, the oral nasal display anatomical changes relationship [8, 9]. Simple three-dimensional imaging techniques, at any time from different angles and different directions of cleft lip and palate sites, were observed and analyzed with good reproducibility. Currently, three-dimensional ultrasound as a screening test has proven to be a feasible screening tool.

6. Conclusions

In summary, two-dimensional ultrasound and three-dimensional ultrasound have the same display rate for cleft lip. During prenatal examination, if a cleft lip is found, three-dimensional ultrasound should be used to further screen for cleft palate deformity. The genetic risk of cleft palate is high, and subsequent treatment is more complicated. Correct diagnosis is very important and can provide important evidence for termination of pregnancy. Three-dimensional ultrasound can show the structure of the palate that is difficult to display with conventional two-dimensional ultrasound, which significantly improves the detection rate of prenatal fetal cleft lip and palate, especially in the diagnosis of cleft palate, which has greater advantages than two-dimensional ultrasound examination and is worthy of clinical promotion and application.

Data Availability

No data were used to support this study.

Conflicts of Interest

The authors declare no conflicts of interest.

References

[1] A. Hrkac Pustahija, I. Horvatic, K. Galesic, and M. Zivko, "[Value of ultrasound-guided percutaneous renal biopsy in diagnosis of the renal diseases]," *Acta Medica Croatica Casopis Hravatske Akademije Medicinskih Znanosti*, vol. 61, no. 4, pp. 399–403, 2019.

[2] S. Wu, "A traffic motion object extraction algorithm," *International Journal of Bifurcation and Chaos*, vol. 25, no. 14, Article ID 1540039, 2015.

[3] J. H. Fleurke-Rozema, K. van de Kamp, M. K. Bakker, E. Pajkrt, C. M. Bilardo, and R. J. M. Snijders, "Prevalence, diagnosis and outcome of cleft lip with or without cleft palate in The Netherlands," *Ultrasound in Obstetrics and Gynecology*, vol. 48, no. 4, pp. 458–463, 2016.

[4] M. H. N. G. Abreu, K. H. Lee, D. V. Luquetti, and J. R. Starr, "Temporal trend in the reported birth prevalence of cleft lip and/or cleft palate in Brazil, 2000 to 2013," *Birth Defects Research Part A: Clinical and Molecular Teratology*, vol. 106, no. 9, pp. 789–792, 2016.

[5] C. L. Werker, H. de Wilde, A. B. Mink van der Molen, and C. C. Breugem, "Internationally adopted children with cleft lip and/or palate: a retrospective cohort study," *Journal of Plastic, Reconstructive & Aesthetic Surgery*, vol. 70, no. 12, pp. 1732–1737, 2017.

[6] S. Wu, M. Wang, and Y. Zou, "Research on internet information mining based on agent algorithm," *Future Generation Computer Systems*, vol. 86, pp. 598–602, 2018.

[7] G. A. Justin and S. E. Brietzke, "Cleft lip and cleft palate surgery: malpractice litigation outcomes," *Cleft Palate Craniofac J*, vol. 54, no. 1, p. 75, 2016.

[8] J. M. Llanes, "Maternal risk factors associated with the development of cleft lip and cleft palate in Mexico: a case-control study," *Iranian Journal of Otorhinolaryngology*, vol. 29, no. 4, pp. 189–195, 2017.

[9] S. Wu, M. Wang, and Y. Zou, "Bidirectional cognitive computing method supported by cloud technology," *Cognitive Systems Research*, vol. 52, pp. 615–621, 2018.